Available online at www.scholarsresearchlibrary.com

Scholars Research Library

Archives of Applied Science Research, 2012, 4 (1):111-127
(http://scholarsresearchlibrary.com/archive.html)

ISSN 0975-508X
CODEN (USA) AASRC9

Anisotropic Mechanical Parameters; Microscopic, Thermal and XRD Studies of Ternary Eutectic Composite Phases Sn-Pb-Cd

Arun K. Sharma, Parshotam Lal, B. K. Gandotra, R. Kant and B. L. Sharma*

Department of Chemistry, University of Jammu, Jammu, India

ABSTRACT

Anisotropic mechanical parameters of eutectic composite Sn-Pb-Cd specimens grown at variable growth rate follow the Weibull probability distribution curve, since the microstructural parameters structuring the specimens by variable anisotropic growth are found obeying the Weibull distribution. Evidentially, the curve exhibits two cut -off points corresponding to a lower strength limit in the slow and fast growth regions and an upper strength limit in the moderate growth region. Investigative evidences indicate the linear variation of the mechanical parameters in the slow and fast growth regions and their nonlinear nature in the moderate growth region over the entire experimental growth range. The latter is equivalent to the theoretical strength of the composite, since the microstructural parameters in the moderate growth region express their proximity obedience to the Guass distribution. Of greater interest is the moderate anisotropic growth velocity (~2.98×10^{-7} $m^3 s^{-1}$) that strengthens the composite specimen three- to four-fold of its isotropic growth affined in an ice bath (~273K) and manifold superior to its constituent phases irrespective of the growth mode. Vickers microhardness of composite specimens encompassing the experimental growth range also offers supporting evidence to the essence of the Weibull distribution curve. Mechanical parameters accomplishing microhardness data are comprehensively extracted, that signify the occurrence of plastic deformation. Growth habits and thermal stability of eutectic composite phases are ascertained using SEM and DSC. X-ray diffraction studies affirm eutectic composite to be a terminal solidus solution of physically distinct and mechanically separable phases.

Keywords: Alloy, crystal growth, hardness, microstructure.

INTRODUCTION

An attractive research enticement towards composites arises from their unique properties, particularly when their constituent phases are geometrically oriented to one another in some anisotropic manner [1-5]. Anisotropically grown composites constitute an efficient class of competent candidates for the construction and further development of supersonic aircraft, space vehicles, high pressure tanks, for which strength properties are required that cannot be provided

by the existing homogeneous materials [6-9]. Composite materials are equally important in other fields and can yield terrific benefits in most industries. The well known example is the decreased fuel consumption in the new Boeing 787 dreamliner which has been designed with light weight, composite fuselage and wings [9-11]. Currently, the femoral stem is constructed from Co-Cr-Mo, Co-Ni-Cr-Mo and Ti-Al-V alloys in preference to stainless steels [3]. Most metallic permanent magnets are made of alnico alloys, whereas quasi binary composite NiSb-InSb finds a representative example in electronics [6,8]. Natural materials and engineering materials are both micro composites, since the properties are achieved from a very fine dispersion of the phases, for which high resolution electron microscopy is required to resolve separate phases [6,8,12]. The 'composite idea' can be related also to the macroscale, since this is particularly relevant to engineering products that may consist of two or more physically distinct and mechanically separable materials and their flux in combination to give performance in-service enticing superiority over the constituent materials [7-12].

In view of peculiar and encouraging societal compatibility, the present investigation is conducted with an aim to explore the anisotropic mechanical parameters of the eutectic composite Sn-Pb-Cd at both macro and micro levels. The parameters of the composites are interpreted on the basis of the inter-lamellae relationship established by examining its specimens, obtained at different growth rates, under scanning electron microscope. The main impetus of the work is the ability to put strong stiff lamellae in the right place, in the right orientation with right volume fraction, since the acceptability of the composite materials technology lies in the concept that the modal product must exhibit properties which are superior in some specific respects, to the properties of the constituent materials. An anisotropically controlled growth from the melt, is a complex phenomenon and a considerable judgment is imperative to evaluate the quality of both theoretical and experimental results because the modal product designed by this process, manifests a large diversity of morphologies. The article would explain how mechanical parameters of a particular combination of metals in eutectic composite, exhibit predominance over homogeneous constituent materials.

MATERIALS AND METHODS

The eutectic composite Sn-Pb-Cd was prepared in a Pyrex tube by weighing a proper amount of purity 99.999% Sn [Alfa Aesar, AR, mp 510.0 K, Δ_f H=7.15 kJmol^{-1}], 99.999% Pb [Alfa Aesar, AR, mp 602.0 K, Δ_f H=4.55 kJmol^{-1}] and 99.999% Cd [Alfa Aesar, AR, mp 591.0 K, Δ_f H=6.12 kJmol^{-1}] shots with 51wt% Sn, 31wt%Pb and 18wt% Cd. The ampoule tube was sealed under vacuum to avoid oxidation and infused in a furnace set at a temperature ~ 773K for alloying Sn, Pb and Cd metals. Homogeneity of the alloy was ensured by heat-chill process keeping the temperature of the heater (air oven) ~ 573 K and that of the cooler (water bath) ~ 298 K. The composition of the alloy was ascertained from its melting temperature 429.0K obtained by DSC (LINSEIS), closely approaching the literature value [13]. Likewise, the enthalpies of fusion, and melting temperatures of the constituent metals, attained by the thermal analysis, are cited in the parentheses and found consistent with their literature values [14].

Anisotropic growth of the alloy and its constituent metals from their respective molten states was acquired in the following experimental setup. An experimental sealed Pyrex tube containing half-full melt of the freshly prepared eutectic composite or metal, was clamped to the centre of an empty graduated beaker (volume capacity ~1dm^3) manipulated midmost in an air oven set at a temperature 30K higher than the melting temperature of the sample. The molten mass in the tube was nucleated by circulating silicone oil, at 16 different intervals spanned in the time range of 5-60 minutes, from the oil reservoir perforated at ~300K. The melt in the tube started

nucleating when the rising level of the oil just touched the bottom of the tube. Several samples of the eutectic composite and its constituent metals were grown anisotropically at different but nearly constant growth rates determined by circulating approximately the same volume of the oil for the aforementioned intervals.

Isotropic growth was achieved by immersing an experimental Pyrex tube containing the eutectic or noneutectic melt in an ice bath maintained at ~273K. The growth being instantaneous in nature, is presumed of zero order. Likewise, a good many samples of Sn-Pb-Cd composite phases, for the isotropic growth were solidified for observations.

The experimental samples after dimensions' measurement, were subsequently subjected to tensile, modulus of rupture (flexural strength) and compressive tests in a VEB Thuringer Industrie Werk Rauenstein Tensometer, whereby, a steadily increasing load would determine the rupture force of an experimental sample until it shows no ability for further resistance.

Indentations were induced on selected points chosen diagonally on variable anisotropically grown composite specimens at room temperature (~300K) using a Vickers microhardness tester attached to an incident-light metallurgical research microscope in the applied load ranging from $10x10^{-2}$ - 100×10^{-2} N. For each test, a very small diamond indenter having pyramidal geometry was forced into the surface of a specimen at room temperature and the size of the indent was found growing with increasing applied load.

The specimens grown anisotropically and isotropically were polished at room temperature following a procedure similar to that adopted for analogous problem [9,15]. To reveal the microstructure, a thin layer of the specimen etched in ferric chloride was mounted on stub with gold-coated holder and examined under a scanning electron microscope for micro growth observations. Lots of samples of each specimen were viewed in this manner and the growth habits of the growing phases during solidification at different growth rates were accordingly photographed.

The X-ray diffraction patterns obtained of the experimental composite phases were recorded with Diffractometer System-XPERT=PRO using CuKα radiation of wavelength 1.5408 Å at room temperature.

The methodology is accomplished with the following analytical approach.

Mechanical parameters of the eutectic composite phases for moderate anisotropic and isotropic modes of growth computed by the following standard relations including Vickers hardness [2,3,16] are presented in Table 1:

(i) tensile strength, T_{rup}

(ii) compressive strength, σ_{rup}

$$\left.\begin{matrix}\text{(i)}\\\text{(ii)}\end{matrix}\right\} = \frac{P}{\pi r^2} \qquad (1)$$

(iii) modulus of rupture, Y_{rup}

$$= \frac{PL}{\pi r^3} \qquad (2)$$

(iv) Vickers hardness, H_v

$$= \frac{1.8544\ P}{d^2} \qquad (3)$$

where P is the applied load in Newton force; L, r and d respectively are the span, radius of the specimen, and average diagonal length of the indentation mark in meters. In these relations, the parameters P and r differ in their magnitudes and depend on both the size of the specimen being tested and the nature of the test, whereas d varies with the size of the cracks. The relationship of the aforementioned mechanical parameters of the eutectic composite Sn-Pb-Cd specimens obtained by variable mode of solidification, with their microstructural growth parameters is depicted in Fig.1 which follows an identical form of Weibull probability distribution curve. Evidentially, the curve has two cut-off points dividing the plot into three regions, namely, (i) slow growth region, (ii) moderate growth region and (iii) fast growth region. Likewise, the dependence of Vickers microhardness, determined by a constant load of $50x10^{-2}$ N for a specified interval of 10s to elaborate the resistance of the eutectic composite Sn-Pb-Cd to localized plastic deformation, on anisotropic growth velocity also evidences the essence of Wiebull distribution curve (Fig. 2) exhorting the strength –growth relationship. Figure 3a reveals the growth habits of the eutectic composite phases experienced in an ice bath (~273K) that at a large kinetic undercooling the lamellae formed are of short size, aggressive, disconnected, crossing each other and showing no matrix relationship. These lamella habits, in fact, arise from splitting of the main single lamella into separate single lamellae or groups of single lamellae, apparently leading to the distorted morphology (Fig. 3b). However, the growth habits of the eutectic composite phases gradually structure themselves to nonaggressive, attaching and parallel to each other reinforcing the matrix with decreasing kinetic undercooling (Fig. 3c).

An entirely distinct lamellar microstructure (Fig. 3d) of the alloy is obtained at the anisotropic growth velocity (~ 2.98 x $10^{-7}m^3s^{-1}$) determined by setting the flow-interval of silicone oil at 5.0 $x10^{-4}m^3$ for 28 min, that enhances the hardness of the alloy to its optimum value in the present investigation. In the lamellar microstructure, some of the unfavorably oriented lamellae in the eutectic grains with high configuration energy grew out perpendicularly to the solidus-liquidus interface leaving other lamellae with orientations close to low configuration energy to grow in an aligned preferred crystallographic morphology. The growth habits of the eutectic composite phases producing the rod-like lamellar microstructure from the melt, present their relationship with the moderate growth velocity. In a melt, when one of the eutectic phases, usually the rich one, grows, the vicinal melt region acquires richness in the other phase, the first phase continues its growth as a lamella unless and until the other phase nucleates at a certain supersaturation. This is another supercrescent lamella growing over that of first phase, which would also continue till another supercrescent lamella of the other phase enriching the melt, appears on it. Thus, the supercrescent lamella growth from the melt produces a complete lamellar microstructure of the eutectic composite called modal product. The growth front of the solidus-liquidus interface structure in the experimental tube, interior and the rising level of silicone oil to its exterior seem advancing nearly with the same pace in a cohesive manner effectively decreasing the kinetic undercooling which balances the undercooling due to composition, and originating lamella length. Accordingly, the growth process produces long lamellae with undamaged surface (Fig. 3e) which are embedded parallel to each other in an attaching and nonaggressive unidirectional lamina (Fig.3d). The mathematical model for the rod-like growth of the eutectic systems has been developed elsewhere [17] . In the directional growth, the metals Sn, Pb and Cd grew out as lamellar cells where each cell crystallized either from the bulk of the melt or through secondary nucleation. Figure 3f likewise, represents the short lamellae of the eutectic composite at growth velocity ~2.55 x $10^{-7}m^3s^{-1}$.

Table 1. Mechanical parameters* of eutectic composite phases at moderate anisotropic growth (~2.98 x 10^{-7} m^3s^{-1}) and isotropic growth (~273 K) rates

S.No.	specimen	modulus of rupture Y_{rup}(MPa)	tensile strength T_{rup}(MPa)	compressive strength σ_{rup}(MPa)	elongation percentage in tensile test
1.	**Sn-Pb-Cd eutectic alloy** anisotropic growth isotropic growth	 98.40 23.20	 106.30 29.40	 119.80 36.10	 8.40 5.94
2.	**Sn** anisotropic growth isotropic growth	 8.40 6.10	 10.28 7.90	 11.30 9.40	 17.50 15.30
3.	**Pb** anisotropic growth isotropic growth	 7.80 6.60	 10.28 8.50	 10.90 9.20	 14.30 11.70
4.	**Cd** anisotropic growth isotropic growth	 4.30 3.20	 5.40 4.60	 6.50 5.40	 5.78 4.67

***** *Averaged values*

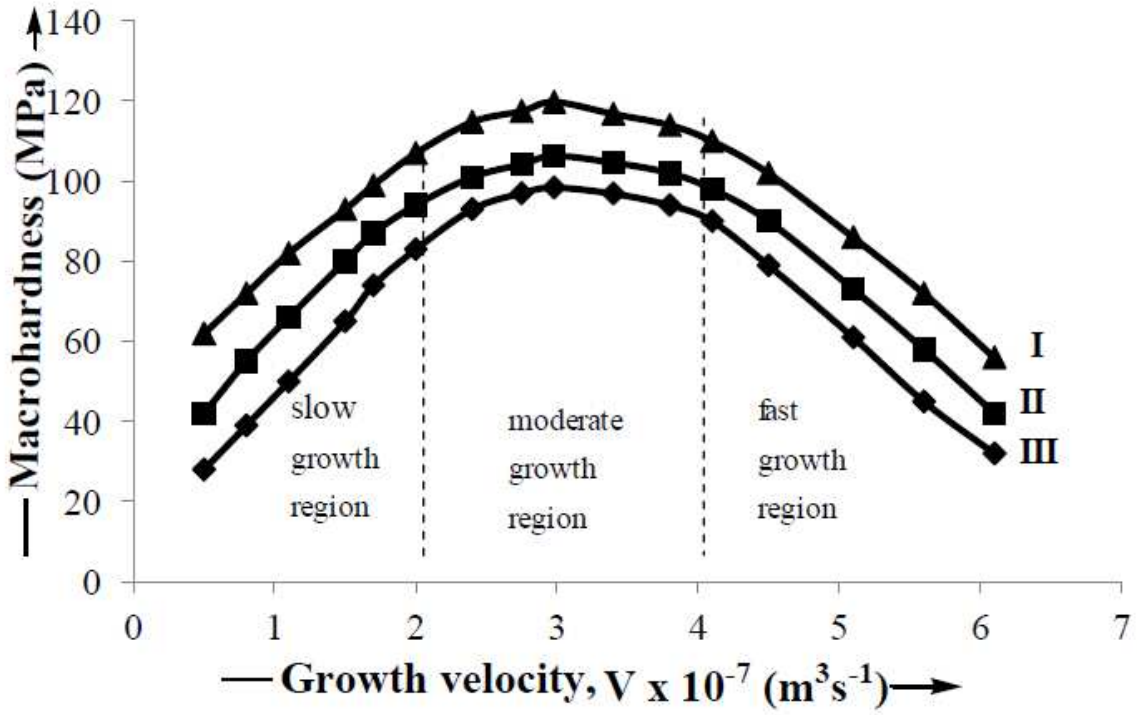

Fig. 1. Dependence of mechanical parameters of the eutectic composite Sn-Pb-Cd over the entire range of experimental growth velocity: I compressive; II tensile and III modulus parameters.

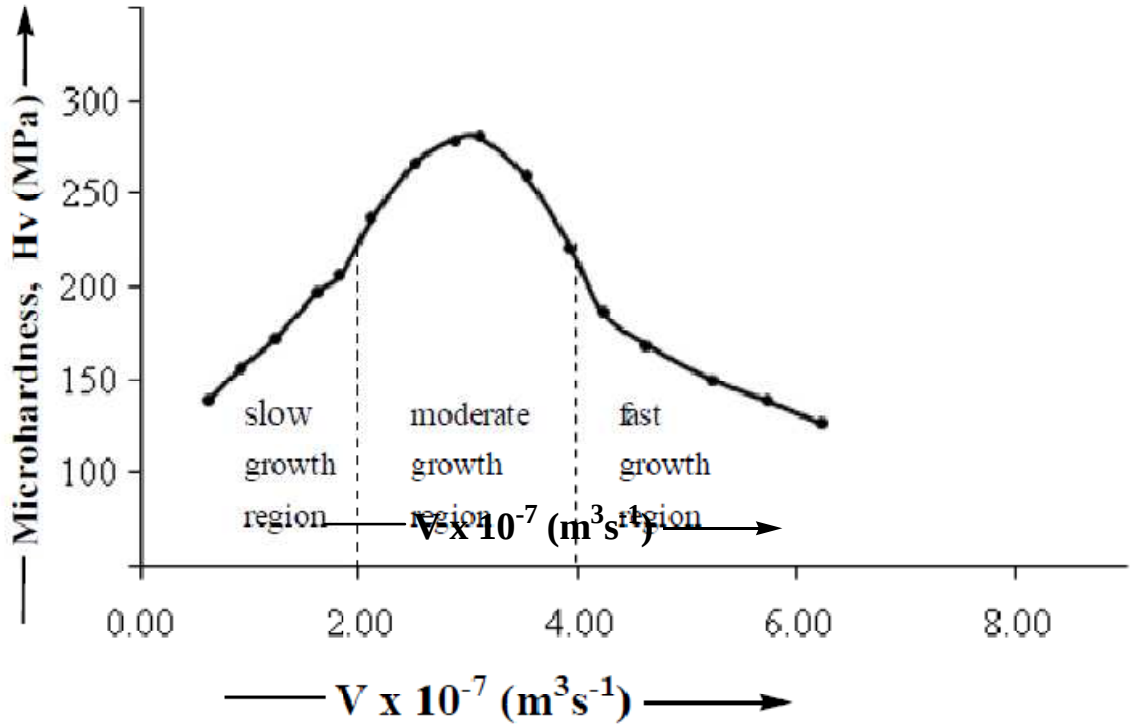

Fig. 2. Variation of microhardness of the eutectic composite Sn-Pb-Cd over the entire range of experimental growth velocity elocity.

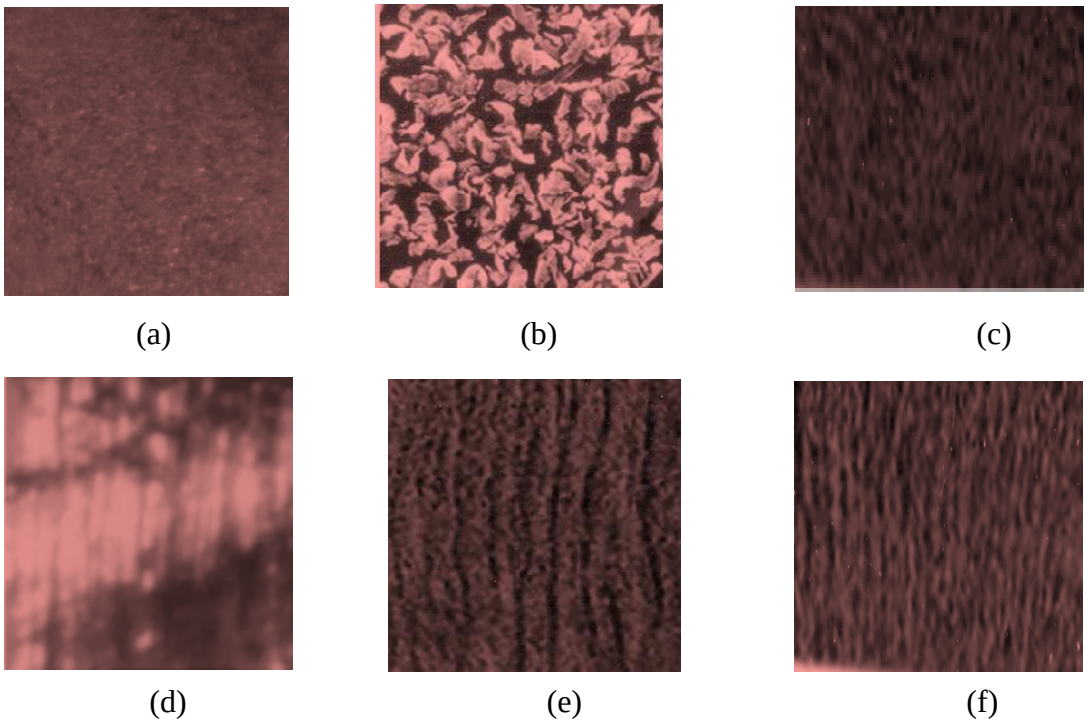

Fig. 3. Microstructures of eutectic composite Sn-Pb-Cd at different modes of solidification (1500x):

(a) isotropic lamellae microstructure in an ice bath at ~ 273K; (b) evolution of lamellae, growth direction from bottom to top at fast growth velocity ~ 5.60 x $10^{-7}m^3s^{-1}$; (c) distorted lamellae, growth direction from bottom to top at slow growth velocity ~ 1.70 x $10^{-7}m^3s^{-1}$, (d) lamellar composite, growth direction from bottom to top at moderate growth velocity ~2.98 x$10^{-7}m^3s^{-1}$ (e) long lamellae at growth velocity ~3.51 x $10^{-7}m^3s^{-1}$, growth direction from bottom to top and (f) short lamellae at growth velocity ~2.55 x $10^{-7}m^3s^{-1}$, growth direction from bottom to top ,.

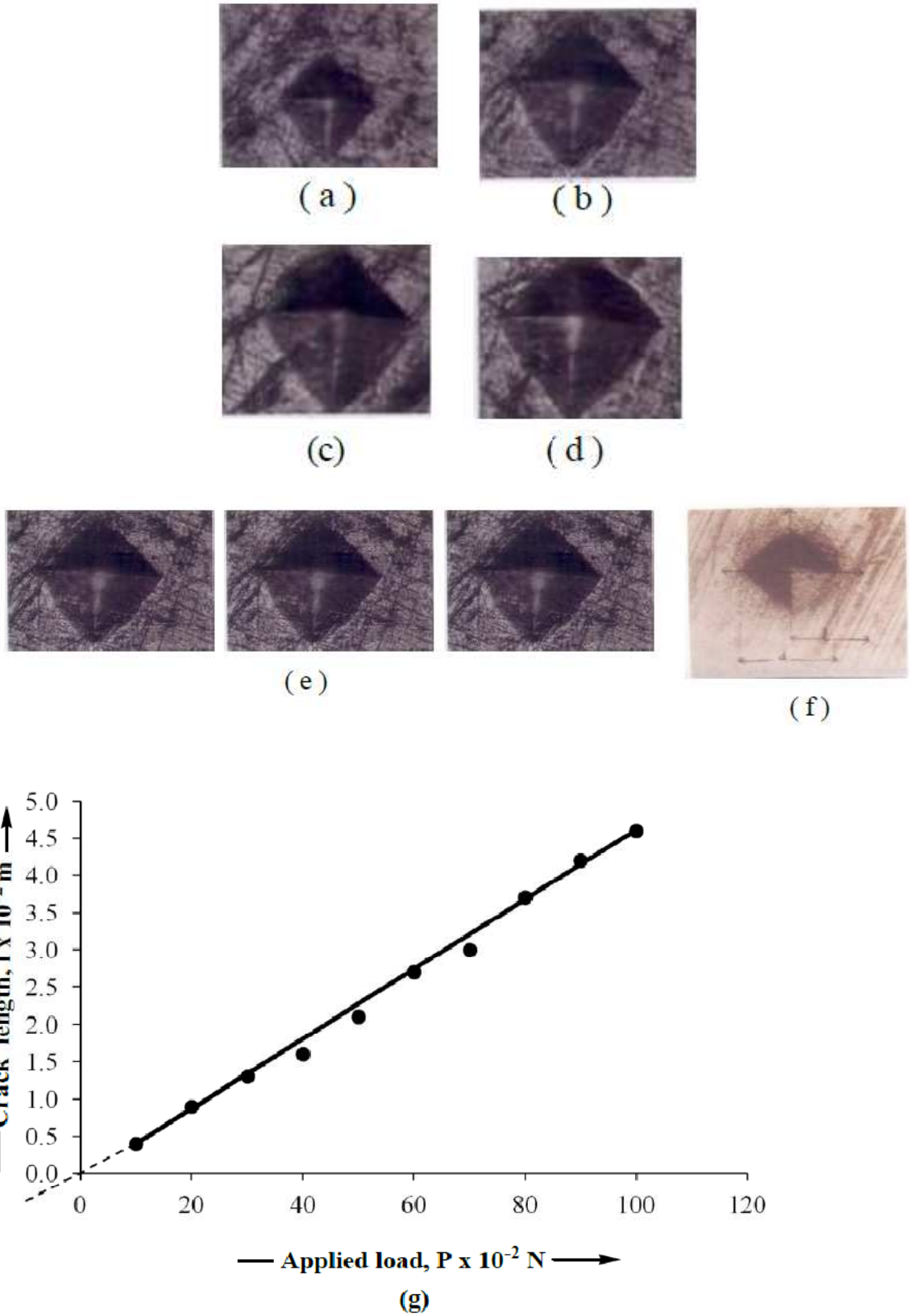

Fig. 4. Photomicrographs showing indentation impressions inflicted on modal eutectic composite Sn-Pb-Cd under variable conditions (625x)

(a) size of the indentation with a load of 10 x 10^{-2} N; (b) size of the indentation with a load of 20 x 10^{-2} N; (c) size of indentation with a load of 40 x 10^{-2} N; (d) size of the indentation with a load of 50 x 10^{-2} N; (e) invariable size of indentation for a constant applied load of 50 x 10^{-2} N at 50, 100, and 150s; (f) measurement of crack length and (g) plot showing variation crack length with applied load.

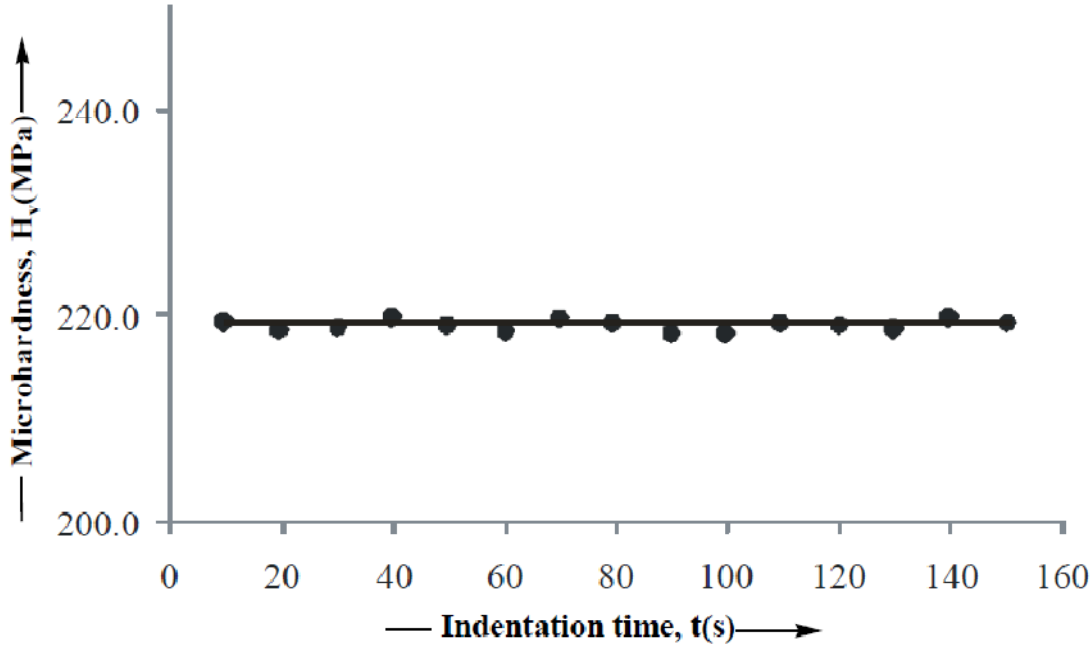

(a)

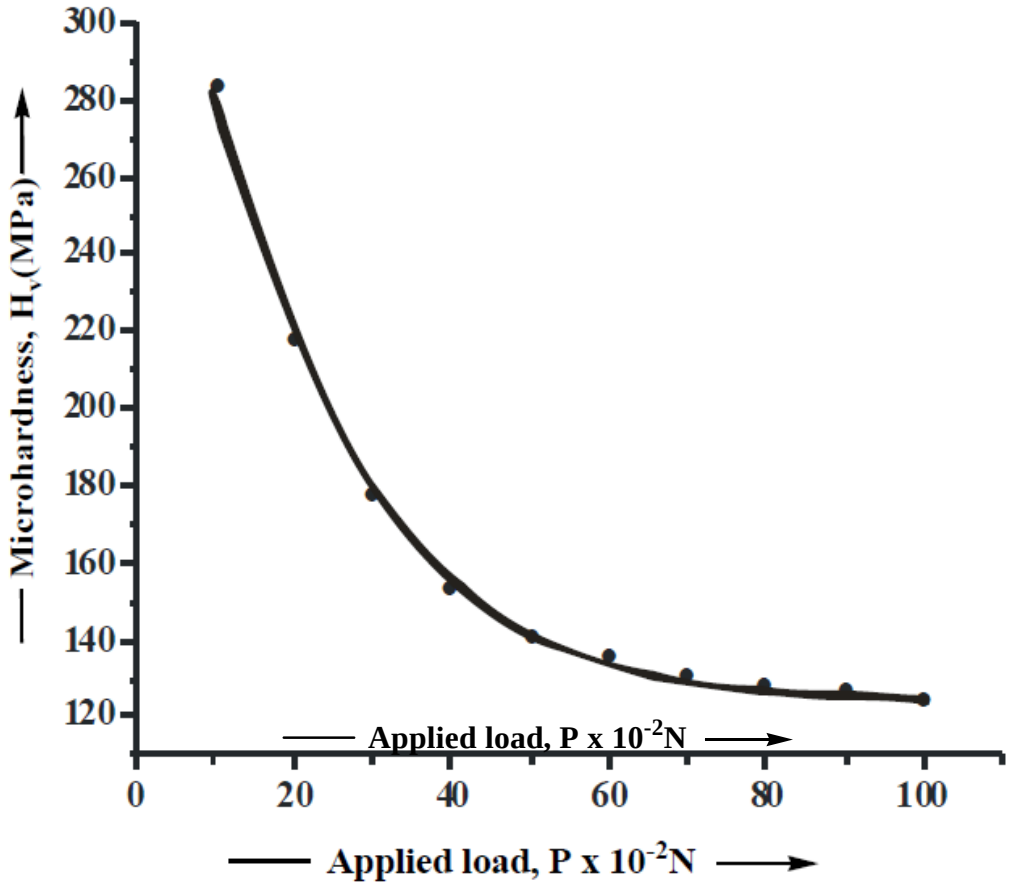

(b)

Fig. 5. Variation of microhardness for the modal Sn-Pb-Cd eutectic composite: (a) linear with variable indentation time for constant applied load P (20 x 10^{-2} N). (b) Nonlinear with variable applied load at constant indentation time, t (10s).

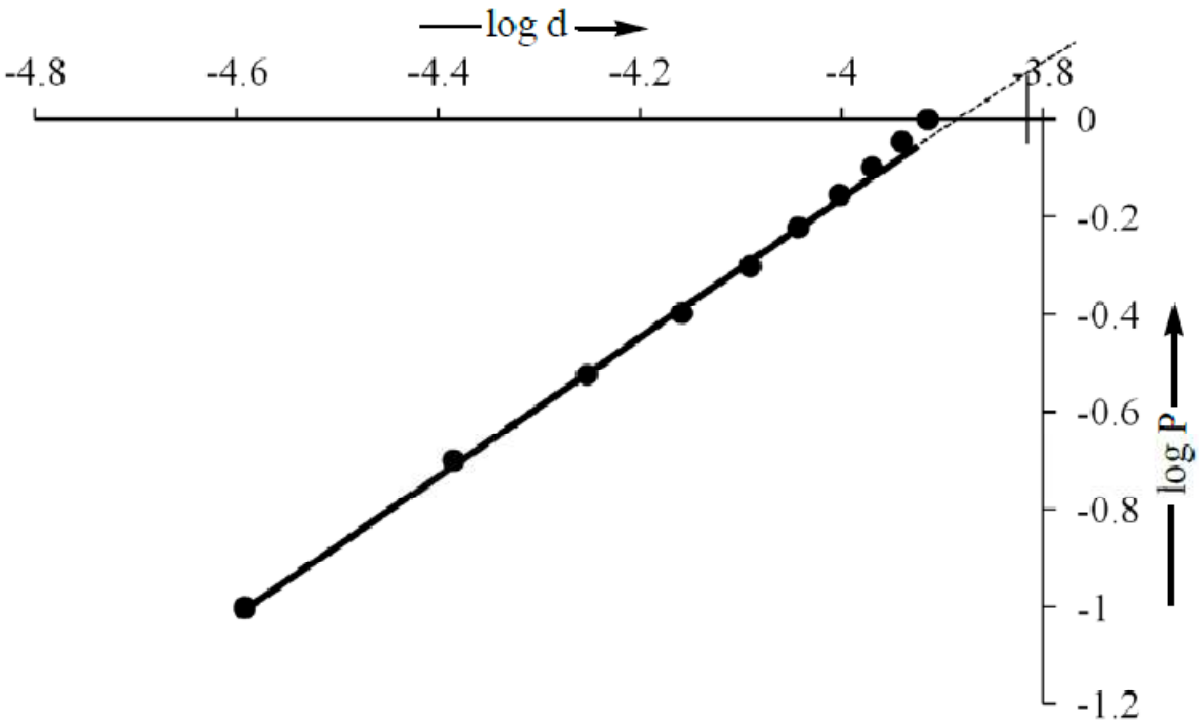
log d
-4.8
-4.6
-4.4
-4.2
-4
-3.8
0
-0.2
-0.4
-0.6
-0.8
-1
-1.2
log P

(a)

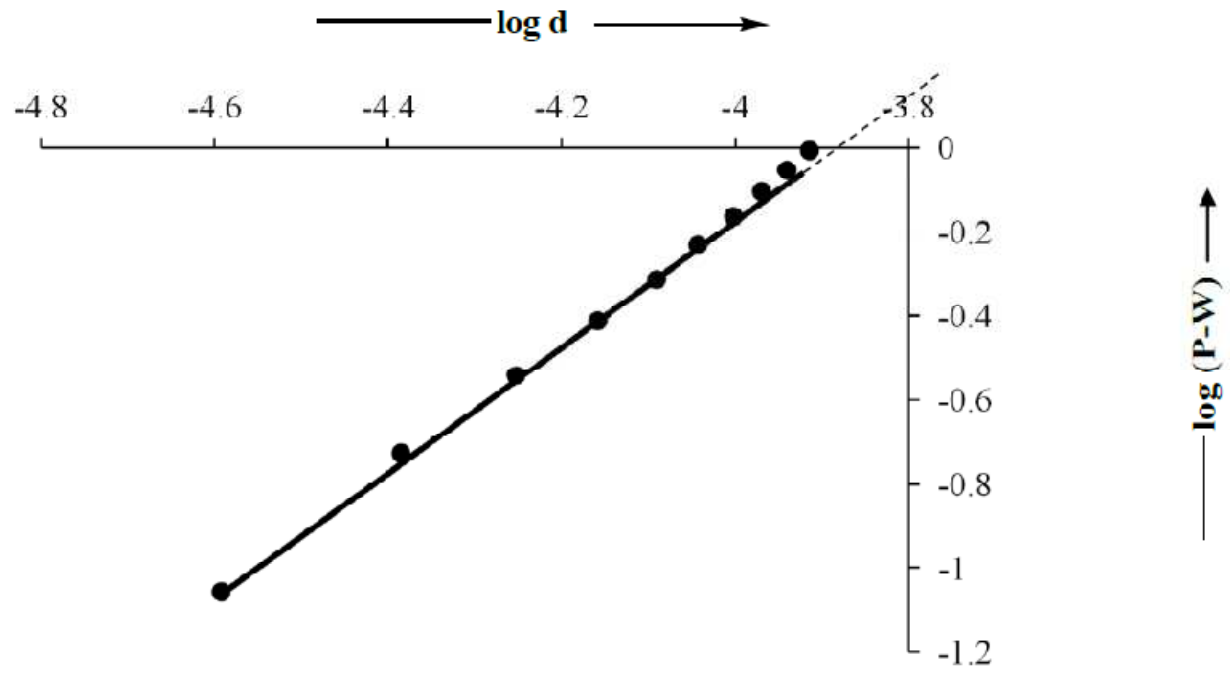
log d
-4.8
-4.6
-4.4
-4.2
-4
-3.8
0
-0.2
-0.4
-0.6
-0.8
-1
-1.2
log (P-W)

(b)

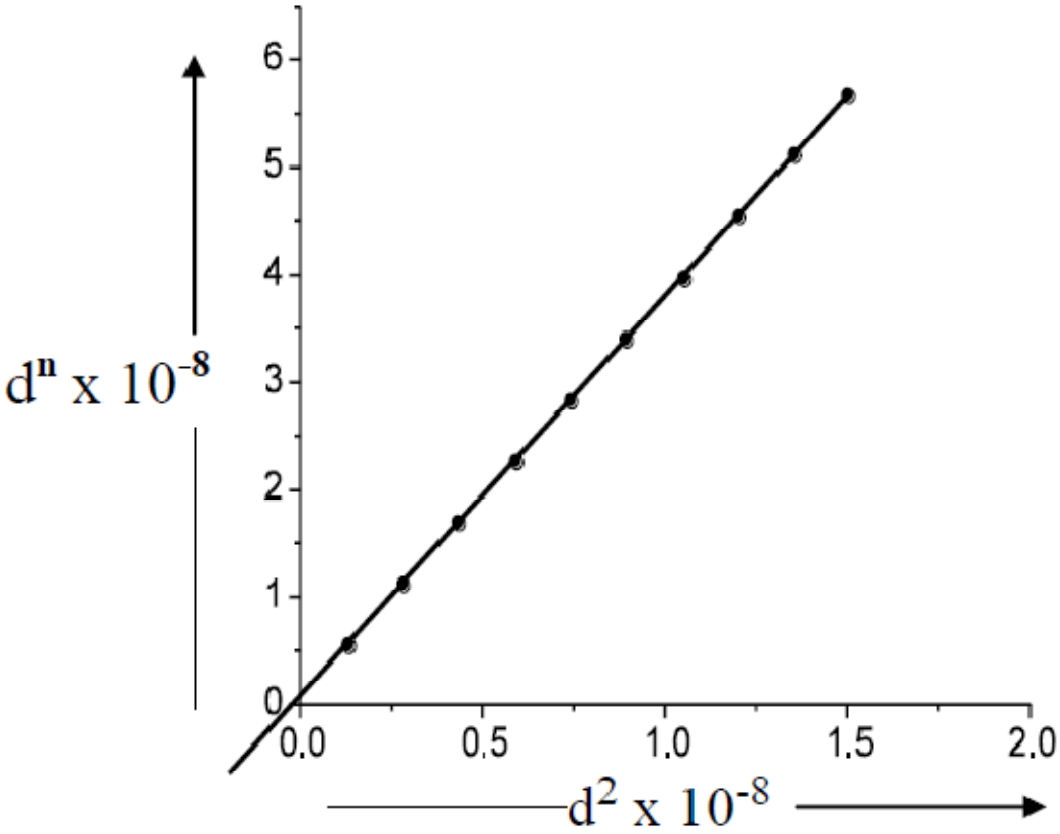

(c)

Fig. 6. Depiction of relations between the variables: (a) log P and log d; (b) log (P-W) and log d and (c) d^n and d^2

Table 2. Micorhardness parameters for modal eutectic composite Sn-Pb-Cd.

S.No	Applied Load P x 10^{-2}N	Crack Length (l x 10^{-2}m)	Fracture toughness K_c ($Nm^{-3/2}$)	Vickers Hardness H_v (MNm^{-2})	Britteness Bi ($10^6 m^{-1/2}$)	Yield strength σ_y (MNm^{-2})
1	10	0.4	56.46	284	5.03	94.67
2	20	0.9	33.46	219	6.55	73.00
3	30	1.3	28.91	178	6.16	59.33
4	40	1.6	28.23	154	5.46	51.33
5	50	2.1	23.47	141	6.01	47.00
6	60	2.7	19.32	136	7.04	45.33
7	70	3.0	19.24	131	6.81	43.67
8	80	3.7	16.05	129	8.04	43.00
9	90	4.2	14.93	127	8.51	42.33
10	100	4.6	14.47	125	8.64	41.67

Figure 4 indicates indentation impressions inflicted on the composite specimens with both variable and invariable experimental loads. In microhardness testing, only well-defined cracks developed during the indentation process were considered for crack measurements. The average crack length of all such cracks was estimated for a particular indentation impression. Figure 4(a-d) shows growing size of an indent with variable applied loads of $10x10^{-2}$, $20x10^{-2}$, $40x10^{-2}$ and $50x10^{-2}$ N respectively. Figure 4e reveals the invariable size of the indent with a constant applied

load of 50 x10^{-2} N, for 50, 100 and 150s. The crack length was measured from the center of the indentation mark to the tip of the crack (Fig. 4f). Consequently, the linear relationship between the crack length and variable applied load is observed and represented in Fig. 4g. The plots 5a and 5b (Fig.5) respectively depict the linear and nonlinear variation of microhardness with the ascent of both indentation time and applied load. The analysis of microhardness is summarized in Fig. 6 and table 2. X-ray of modal eutectic composite Sn-Pb-Cd are distinguished in Fig. 7 and various parameters in XRD data are recorded in Table 3.

Fig. 7. XRD patterns of the eutectic composite Sn-Pb-Cd..

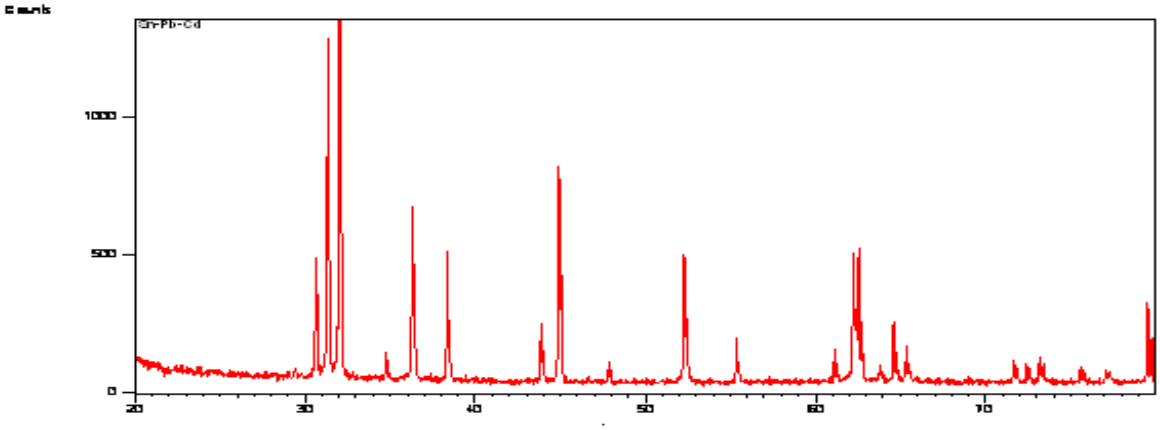

Table 3. XRD data of eutectic composite Sn-Pb-Cd

Pos. [°2TH.]	d-Spacing [Å]	rel. Int. [%]	area [cts*°2Th.]	corresponding atomic planes
30.656	2.9165	36.26	41.55	Sn(200)
31.341	2.8542	99.91	152.80	Pb(111)
32.062	2.7917	100.00	152.66	Sn(101)
34.762	2.5808	8.39	9.62	Cd(100)
36.331	2.4728	51.88	99.10	Pb(200)
38.381	2.3453	33.69	51.48	Cd(101)
43.879	2.0634	16.50	25.21	Sn(220)
44.912	2.0183	61.21	116.91	Sn(211)
47.834	1.9016	6.06	6.94	Cd(102)
52.295	1.7494	36.24	41.53	Pb(220)
55.347	1.6599	12.75	14.61	Sn(301)
61.179	1.5150	4.14	9.49	Cd(103)
62.233	1.4906	37.85	71.50	Cd(113)
62.555	1.4849	38.43	44.04	Sn(112)
63.786	1.4592	4.60	5.27	Sn(400)
64.597	1.4416	17.11	32.32	Sn(321)
64.791	1.4413	8.55	16.14	Sn(321)
65.377	1.4263	5.76	21.77	Pb(222)
s71.658	1.3159	6.21	11.72	Cd(112)
72.417	1.3040	5.78	10.91	Sn(420)
73.394	1.2890	4.93	9.31	Cd(200)
75.584	1.2570	4.67	8.83	Cd(201)
77.093	1.2361	3.63	9.15	Cd(104)
79.528	1.0243	23.02	43.49	Sn(312)

RESULTS AND DISCUSSION

The experimental results strongly emphasize that the mechanical properties (macro- and microhardness) of the eutectic composite,Sn-Pb-Cd are the attributions of the microstructures obtained at different growth rates. The investigative analysis necessarily involves a physical understanding of the relationship between the growth habits (Fig.3) and mechanical parameters (Figs. 1,2 and Table 1) of the eutectic composite Sn-Pb-Cd. A critical examination of Table 1 reveals an important aspect of the investigation that the moderate growth (~2.98 x $10^{-7}m^3s^{-1}$) strengthens the microstructure of the eutectic composite Sn-Pb-Cd approximately three- to four-fold of its isotropic growth (~ 273K) and manifold superior to its constituent phases irrespective of the growth mode whether anisotropic or isotropic. As mentioned earlier, the variation of the mechanical property over the entire experimental growth velocity range follows the Weibull probability distribution curve (Figs. 1 and 2) that acquire two cut-off points which divide the plot into three regions namely: (i) slow growth region; (ii) moderate growth region and (iii) fast growth region.. Figures 1 and 2 indicate that among the growth regions, the moderate growth region appears to be the most probable one for producing the complete lamellar microstructure (modal product) of the eutectic composite(Fig. 3d) wherein microstructural parameters, namely, lamella diameter, lamella length, lamella length distribution, volume fraction of lamellae, and the alignment and packing arrangements of lamellae, seem nearly obeying the Gauss distribution. By virtue of the growth process, the composite (Fig. 3d) manifests mechanical properties which are to that of its isotropic growth in an ice bath (Fig.3a) and its constituent phases (Table 1) which grew out as lamellar cells with aggressive and crossing microstructural parameters producing fragile matrix. The physical significance to be drawn from these plots is that the variation of an anisotropic mechanical property over the entire experimental range of growth velocity furnishes an evidence of its dependence as linear, optimum, and linear respectively in the slow, moderate, and fast growth regions of solidification. The concept implicitly, generates the strength-growth relationship, which follows an identical form of the Weibull distribution curve [5,8,18], since the microstructural parameters follow the distribution, particularly in the slow and fast growth regions (Fig. 3a-c). Eventually, the two cut off points occur on the corresponding curve to a lower strength limit in the slow and fast growth regions, and an upper strength limit in the moderate growth region. The latter is equivalent to the theoretical strength of the lamellae, as the microstructural parameters nearly obey Gauss distribution (Fig. 3d), in the absence of any internal defects or surface flaws which are responsible for reduced strength.

The ascent in macro and micro mechanical modes of the eutectic composite (Figs.1 and 2) in the moderate anisotropic growth region is explained in view of the lamellar growth habits of the eutectic phases from the melt (Fig. 4b). The lamellae are the fibers practically having no density of dislocations, particularly when developed in the moderate growth region in which they are parallel to each other in an attaching and nonaggressive unidirectional lamina (Fig. 4a) reinforcing the matrix where there is a perfect lamella-matrix bond. This leads to an implicit obedience of microstructural parameters to the Gauss distribution that the lamellar growth Fig. 3(d-f) of the eutectic composite expresses higher strength ability over its random growth (Fig. 3a-c) and constituent phases (Table 1), since the lamellae of the modal composite phases are in equilibrium with the matrix resulting in strong lamella-matrix relationship, while Fig.3(a-d) expresses distorted structure of the composite comprising of aggressive, non-attaching and irregular thin lamellae which produce its fragile lamella matrix interdependence. The variable change in spacing, in absence of faults (Figs.3a-c,e,f), is the movement of lamellar faults, which is an evidence for the fault-mechanism [12-18]. It is this movement aspect of the lamellae, not the formation of faults, which is an important factor in controlling the spacing among lamellae. The lamellar cells of the pure eutectic phases would acquire dislocations by virtue of their

growth by fault-mechanism from the melt and consequently, exhibit much lower strength compared to lamellar growth of the alloy. Hardness is actually the structural property of a physical body by virtue of which it resists its permanent deformation. The slight increase in the hardness of the anisotropically solidified pure individual composite phases (Table 1) in comparison with their isotropic growth (~273 K) occurs owing to a linear alignment of the lamellae although having dislocations. These growth habits of the pure phases also result in the morphology for composite's isotropic growth from a strength point of view. Imperatively, the experimental observation that eutectic alloy with isotropic growth, stronger than that of the constituent metals. The Fiber-reinforced composites often include high strength and stiffness on weight basis. The characteristics of the composites are expressed in terms of specific strength and specific modulus parameters, respectively corresponding to the ratio of strength to specific gravity. Consequently, lamella-reinforced composites with exceptionally high specific strengths and moduli, are produced that utilize low-density lamella, and matrix materials [4,5,8].

A comparative study of the macromode strength (Tables1and Fig. 1) reveals that the compressive mode is slightly higher than the tensile which in turn, slightly exceeds the modulus of rupture (σ_{rup}>T_{rup} >Y_{rup}). In view of the strength mode order, an inferential insight may be proposed that the phenomenon of multiphase growth from eutectic melt influences the lamella's length. In the present case, three eutectic phases would solidify as supercrescent lamellae and the length of each metal-lamella gets shortened during the growth process. Since the complete lamella is an attachment of three nonaggressive ductile metal lamellae, the efficiency of the lamellae in stiffening and reinforcing the matrix decreases as the lamella length decreases. Lamella ends play an important role in the fracture of short lamella composites (Fig. 4g) and also in continuous lamella composites (Fig. 4f), since the long lamellae may break down into discrete lengths.

The indentation impressions inflicted on the composite specimens solidified at moderate anisotropic growth (~$2.98\times10^{-7}m^3s^{-1}$) selected in the present work with a constant load of 50×10^{-2} N for indentation times of 50, 100 and 150 s are shown in Fig. 4e. There is practically no change in the size of the indentation mark, as is apparent from the figure itself, and hence in the microhardness. These observations are strongly supported by Fig.5a indicating the microhardness of the eutectic composite to be independent of variation in the indentation time for a constant load of 50 x 10^{-2}N at room temperature and revealing the occurrence of plastic deformation which remains unaffected with variable indentation time.

The nonlinear variation of microhardness with the applied load (Fig.5b) implies that the Vickers hardness, H_v decreases with the increasing applied load until about 60×10^{-2} N and then H_v tends towards saturation, which is full beyond 70×10^{-2} N. This variation can qualitatively be explained on the basis of the penetration depth of the indentor. Since the indentor penetrates only on surface layers at small loads, the effect is more pronounced at these loads. Indented microphotographs with variable applied load (Fig.4a-d) and the plot in Fig.4g offer physical understanding of the observation. However, as the depth of penetration increases, the damage of inner layers becomes more effective to shattering the ability of hardness and ultimately H_v reaches a saturation value that remains constant for further applied load. This is what happens in the range of applied loads, which in the present case, is at and beyond 70 x 10^{-2} N. The type of behavior is consistent with the microhardness increase at loads during early stages of plastic deformation [20], but the variation is contrary to Kick's law that Hv remains constant irrespective of the magnitude of applied load, 'P' and consequently average diagonal length 'd' qualitatively [20-21]:

$$P = k_1 d^n \qquad (4)$$

where Meyer's index $n = 2$, accounts for constant H_v, and k_1 is a constant.

The literature also indicates the decrease and increase of H_v with rising applied load for materials culminating $n < 2$ and $n > 2$ respectively. A plot between log P and log d (Fig.6a) is linear and according to Eq.4, yields n and k_1 for any set of discrete data, the index n being determined by the slope, while k_1 by the intercept, defined as the particular load P that exists at $d = 10^{-3}$m.In the present investigation, n and k_1 respectively obtained by Fig. 6a are 1.64 and 1. 2179 MPa. It is appropriate to recall here that hardness is the ability of a body to resist permanent deformation defined as the ratio W/A, where W and A, respectively are the load in N, and the area of indentation in m^2. Implicit in this definition is the concept that as load P is applied to a specimen, it is partially affected by a smaller resultant pressure, W, which is a function of the material being tested. Obviously, if the portion of resistance is evaluated as a Newtonian resultant pressure of the specimen itself, then it is possible to analyze microhardness data in terms of actual load (P-W) acting on the specimen without undue consideration of the applied load. This concept is called Hays and Kendall hypothesis [22]. The resultant pressure, W of a material thus represents the minimum applied load to cause indentation, as loads less than W will not, by definition, result in plastic deformation. In consequence thereof, Hays and Kendall modified Eq.(4) of Kick's law on the basis of the specimen resistance pressure, W and accordingly, the valid equation is;

$$(P-W) = k_2 d^2 \qquad (5)$$

where k_2 and W are constants. A plot of log (P-W) versus log d of Eq. (5) suggesting the logarithmic index n=2, drawn in Fig. 6b yields the value of the logarithmic index, $n <$ 2,(n=1.6368), thus confirming the validity of the Newtonian resistant pressure theory for the composite specimen, as mentioned earlier, W allows the limiting case to prevail whereat hardness becomes independent of load. Further, the evaluation of W follows the procedure necessarily involving subtraction of Eq. (4) from Eq. (5) which results in:

$$d^n = \left(\frac{k_2}{k_1}\right) d^2 + \frac{W}{k_1} \qquad (6)$$

Analogically, a plot for d^n (n=1.64)versus d^2 (Fig. 6c) yields the slope K_2/K_1 (49.9141) and W/k_1 $2.95\text{x}10^{-8}$ m^2 which K^2 and W are separately calculated from the known value of K_1 determined by the plot 6a, to their respective values 60.7904 MPa and $3.5928\text{x}10^{-2}$ N provided in Table 3 furnishing a compilation of key data on microhardness.

Toughness virtually measures the ability of a material absorbing energy up to fracture. Furthermore, fractureness is a property indicative of material's resistance to fracture when a crack is present.

The crack developed on the composite specimen determines the fracture toughness K_c, which specifies the extent to which fracture stress is applied on a uniform loading by the relation [23,24] :

$$K_c = \frac{P}{\beta l^{\frac{3}{2}}} \qquad (7)$$

where l is the radius of a semicircular radial crack or the crack length measured from the centre of the indentation mark to the crack tip. β is a numerical constant that depends on indentor

geometry. For a Vickers indentor β = 7. However, Eq. (7) yields satisfactory values of the fracture toughness only if l/ ≥ 3 or l/a < 3, respectively for median or radial crack system (Fig. 4f) where 'a' exactly equals half diagonal length, i.e, a = d/2. Table 4 records the values of crack length, l and fracture toughness, K_c for the eutectic composite specimen at different applied loads. Figure 4(g) is a plot between applied load, P and crack length, l indicating the linear dependence of the crack length on the increasing applied load.

Brittleness is an important property, usually termed as the brittleness index B_i, which can be determined from K_c values obeying the relationship [24] :

$$B_i = \frac{H_v}{K_c} \qquad (8)$$

the values of B_i obtained from Eq. (8) for the composite specimen at variable microhardness-fracture toughness ratio are presented in Table 4.

The yield strength of the composite computed from the hardness data at variable applied load using the valid equation [18] for n < 2:

$$\sigma_y = \frac{1}{3} H_v \qquad (9)$$

σ_y values estimated for the composite in the experimental load ranging from 10 x 10^{-2} to 100 x 10^{-2} N for an indentation interval of 10 s are also incorporated in Table 4. All the parameters hereinabove are well computable, and their computation collectively, accomplishes inferential analysis that emphasize the plastic deformation of the eutectic composite Sn-Pb-Cd in the investigation.

The analysis of X-ray diffraction patterns (Fig.7) exhibited by the eutectic composite Sn-Pb-Cd, reveals the sharp lines of body centered tetragonal phases of tin, face centered cubic phases of lead and hexagonal phases of cadmium. These lines are found nearly obeying their inherent atomic intensities observed in the individual X-ray patterns of the constituent metals (Table 3), wherein the diffraction peaks are on the order comparable to their respective lines compiled into powder diffraction files, namely, Sn (04#0673), Pb (04#0686) and Cd (05#0674). This implies that the X-ray diffraction pattern analysis implicitly, inculcates the existence of the eutectic composite as a mechanical mixture of constituent metals simulating weak interactions because of their atomic electronegative character, since no unique diffraction line is exhibited by the eutectic composite. The physical significance of the observations extracted from the X-ray analysis, is that the eutectic is not a solidus solution but a terminal solidus solution.

CONCLUSION

An identical form of the Weibull probability distribution curve resulting-in from the mechanical property-growth relationship presenting the obedience of the microstructure parameters to the distribution, implicitly, exhibits three regions namely slow, moderate, and fast growth regions. Accordingly, the curve exhibits two cut-off points corresponding to lower strength limit and an upper strength limit. The results of mechanical properties in the slow and fast growth regions are found tending each other, whereas uniqueness in the moderate growth region is comprehensively explained vis-avis those of the slow and fast growth regions. Of greater interest is the moderate growth region which produces a complete lamellar microstructure consisting of the lamellae

practically with damage free-surfaces embedded parallel to each other in an attaching and nonaggressive unidirectional lamina where there is a perfect lamella-matrix bond strengthening the eutectic composite two to three times of its anomalous growth and manifold of its constituent phases irrespective of the mode of the growth. Consequently, the eutectic composite, from macro and micro observations, attains optimum hardness at the moderate anisotropic growth velocity ($2.98 \times 10^{-7} m^3 s^{-1}$). The micro hardness of the composite is found independent of the indentation time but does follow show non-linear dependence with variable applied load. The initiation of the crack on the composite specimen with the required minimum load affirms the applicability of the Newtonian theory of its resistance pressure. The generation of the radial cracks by an indentor loaded with pressure ranging from 10×10^{-2} -100×10^{-2}N faciles the procedure to estimate the values of fracture toughness, brittleness index and yield strength of the eutectic composite specimen. The inferential significance of the mechanical parameters extracts the concept that the properties of the composite are superior and possibly unique to the properties of the pure constituent metals particularly, when its modal product is achieved by moderate anisotropic growth. Moreover, the physical understanding of the X-ray studies defines the eutectic composite to be a terminal solidus solution constituent metals stimulating weak interactions at their atomic level.

REFERENCES

[1] D Hull, TW Clyne, An Introduction to Composite Materials, 2nd Edition (Cambridge University Press, New York, **1996**).
[2] BL Sharma, Mater. Chem. *Phys.*, **2003**, **78**, 691.
[3] WD Callister Jr., Materials Science and Engineering An Introduction, 6th Edition (John Wiley & Sons, Inc., **2006**).
[4] WD Callister, DG Rethwisch, Composites: Polymer-Matrix composites. Fundamentals of Materials Science and Engineering, 3rd Edition (Hoboken, NJ: Wiley, **2008**).
[5] D Hull, TW Clyne, An Introduction to Composite Materials, 3rd Edition (Cambridge University Press) (**2008**).
[6] W Albers, Preparative Methods of Solid State Chemistry, edited by Hagen Muller (Academic Press, New York, **1972**).
[7] DE Ovesienko, GA Alfinstev, Crystal Growth, Properties and Application, 2,ed. Arizumi T (Springer-Verlag, Berlin, Heildberg, New York, **1980**).
[8] D Hull, An Introduction to Composite Materials (Cambridge University Press, Cambridge, **1985**).
[9] R Caram, WR Wilcox , J. Mater. Proc. Man. Sci. **1992**, **1**, 56.
[10] Smock, Doug "*Boeing 787* Dreamliner Represents Composites Revolution." Design News. Reed Business (**2008**).
[11] Sofge, Eric "Boeing's News 787 Dreamliner: How it Works." *Popular Mechanics* (**2010**).
[12] BL Sharma, S Tandon, S Gupta, *Cryst. Res. Technol.* **2009**, **44**, No. 3, 258.
[13] CR Tottle, An Encyclopedia of Metallurgy and Materials, LXVI, Macdonald and Evans Ltd.,(Great Britain, **1984**).
[14] DR Lide, CRC Handbook of Chemistry and Physics, 90th Edition (CRC Press, London, **2009**).
[15] R Caram, M Banan, WR Wilcox, *J. Cryst. Growth* **1991**, **114**, 249.
[16] BL. Sharma, S Gupta, S Tandon, R Kant, *Mater Chem. Phys*., **2008**, **111**, 423.
[17] R Caram, S Chandrasekhar, W R Wilcox, *J. Cryst. Growth* **1990**, **106**, 294.
[18] JD Hunt, K A, Jackson, *Trans. AIME* **1966**, **236**, 843.
[19] C A Brookes, Institute of Physics Conference Series, **1986**, **75**.
[20] BL Sharma, *J. Alloys Compd*. **2004**, **385**, 74.

[21] KJ Pratap, VH Babu, *Bull. Mater. Sci*. **1980**, **2**, 43.
[22] C Hays, E G Kendall, *Metallography*, **1973**, **6**, 275.
[23] B R Lawn, E R Fuller, *J. Mater. Sci*. **1975**, **9**, 2016.
[24] K Nihara, R Morena, DPH Hasselman, *J. Mater. Sci. Lett*. **1982**, **1**, 13.